



Mahler, D. H., Rozema, L., Fisher, K., Vermeyden, L., Resch, K. J., Wiseman, H. M., & Steinberg, A. (2016). Experimental nonlocal and surreal Bohmian trajectories. *Science Advances*, 2(2), [e1501466]. DOI: 10.1126/sciadv.1501466

Publisher's PDF, also known as Version of record

License (if available):
CC BY-NC

Link to published version (if available):
[10.1126/sciadv.1501466](https://doi.org/10.1126/sciadv.1501466)

[Link to publication record in Explore Bristol Research](#)
PDF-document

This is the final published version of the article (version of record). It first appeared online via Science at <http://advances.sciencemag.org/content/2/2/e1501466>. Please refer to any applicable terms of use of the publisher.

University of Bristol - Explore Bristol Research

General rights

This document is made available in accordance with publisher policies. Please cite only the published version using the reference above. Full terms of use are available:
<http://www.bristol.ac.uk/pure/about/ebr-terms>

Experimental nonlocal and surreal Bohmian trajectories

Dylan H. Mahler,^{1,2*} Lee Rozema,^{1,2} Kent Fisher,³ Lydia Vermeyden,³ Kevin J. Resch,³ Howard M. Wiseman,^{4*} Aephraim Steinberg^{1,2}

2016 © The Authors, some rights reserved; exclusive licensee American Association for the Advancement of Science. Distributed under a Creative Commons Attribution NonCommercial License 4.0 (CC BY-NC). 10.1126/sciadv.1501466

Weak measurement allows one to empirically determine a set of average trajectories for an ensemble of quantum particles. However, when two particles are entangled, the trajectories of the first particle can depend nonlocally on the position of the second particle. Moreover, the theory describing these trajectories, called Bohmian mechanics, predicts trajectories that were at first deemed “surreal” when the second particle is used to probe the position of the first particle. We entangle two photons and determine a set of Bohmian trajectories for one of them using weak measurements and postselection. We show that the trajectories seem surreal only if one ignores their manifest nonlocality.

INTRODUCTION

The concept of a trajectory, the path followed by a particle, is ubiquitous in classical mechanics. In orthodox quantum mechanics, however, a particle does not follow a trajectory, because it does not have a simultaneous position and momentum. Nonetheless, it is possible to re-interpret the quantum formalism as describing particles following definite trajectories, each with a precisely defined position at each instant in time. However, in this interpretation, called Bohmian mechanics (1–4), or the de Broglie–Bohm interpretation (5, 6), the trajectories of the particles are quite different from those of classical particles, because they are guided by the wave function. This allows for phenomena such as double-slit interference, as has been investigated experimentally for single photons (7). Note that this is very different from the Feynman path formalism of quantum mechanics (8), where the transition probability between two points in phase space is calculated using all possible paths between those two points. In contrast to the Feynman formalism, Bohmian mechanics says that each quantum particle in a given experiment follows a trajectory in a deterministic manner. Thus, much of the intuition of classical mechanics is regained.

As with any interpretation of quantum mechanics, the experimental predictions of Bohmian mechanics are the same as those in the operational theory. The stochastic nature of measurement outcomes for which quantum mechanics is famous is ascribed to ignorance about the initial configuration of the particle(s) in the experiment, an uncertainty that is described precisely by the wave function prepared by the experimenter (1–4, 6, 9). This tidily allows features of operational quantum theory, such as the Heisenberg uncertainty principle, to be explained within the Bohmian formalism. A consequence of this is that the trajectory of a single Bohmian particle cannot be observed in an experiment on that particle; any measurement of a particle’s position changes the wave function and thus the guiding potential that the particle experiences. Note that this change does not occur through a “collapse” that is added

to the theory (as in other interpretations of quantum mechanics) but is rather due to the evolution of the global wave function, describing the interaction of the particle of interest with a measurement device that has its own Bohmian degrees of freedom. Although a single particle’s trajectory cannot be directly observed, a set of trajectories of an ensemble of particles can be mapped out. This can be done by making a so-called weak measurement of the momentum of a particle at a given instant in time. The weakness ensures that the system is not disturbed appreciably, so that it is sensible to make a subsequent measurement of position. Repeating the experiment many times, one can calculate the average momentum as a function of position. This entire process can then be repeated at many instants in time, allowing a set of average trajectories to be reconstructed. It was shown by Wiseman (9) how these trajectories, in the limit of very weak measurements, correspond exactly to the trajectories obtained from the Bohmian interpretation.

To explain nonlocal phenomena such as Bell nonlocality (10), any realistic interpretation of quantum mechanics must also be nonlocal, and Bohmian mechanics is no exception (2). This can be seen in the Bohmian velocity law (shown later), where the velocity of a particle can depend explicitly on the position of a second particle, even when the particles are far apart and not interacting by any conventional mechanism and even though the second particle may be influenced, independently of the first particle, by the apparatus chosen by the experimenter.

Here, as proposed by Braverman and Simon (11), we experiment on two entangled particles (photons) and map out the trajectories of one of them as it traverses a double-slit apparatus. We show that the trajectories of this first particle (and therefore both its position and its velocity) are indeed affected by an externally controlled influence on the distant second particle. For some choices of that control, the second particle in our experiment can be used to determine through which slit the first particle has gone. Englert, Scully, Süssmann, and Walther (ESSW) (12) asserted that in the presence of such a Welcher Weg measurement (WWM) device, the particle’s Bohmian trajectories can display seemingly contradictory behavior: There are instances when the particle’s Bohmian trajectory goes through one slit, and yet the WWM result indicates that it had gone through the other slit. ESSW concluded that these trajectories predicted by Bohmian mechanics could not correspond to reality and they dubbed them “surreal trajectories.” This serious assertion was discussed at length in the literature (13–17), after which a resolution of this seeming inconsistency was proposed by Hiley *et al.*

¹Centre for Quantum Information and Quantum Control, Department of Physics, University of Toronto, 60 Saint George Street, Toronto, Ontario M5S 1A7, Canada.

²Canadian Institute for Advanced Research, 180 Dundas Street West, Suite 1400, Toronto, Ontario M5G 1Z8, Canada. ³Institute for Quantum Computing and Department of Physics and Astronomy, University of Waterloo, 200 University Avenue West, Waterloo, Ontario N2L 3G1, Canada. ⁴Centre for Quantum Dynamics, Griffith University, Brisbane, Queensland 4111, Australia.

*Corresponding author. E-mail: dmahler@physics.utoronto.ca (D.M.); h.wiseman@griffith.edu.au (H.W.)

(18). Here, we present an experimental validation of this resolution, in which the nonlocality of Bohmian mechanics comes to the fore.

THEORY

The de Broglie–Bohm dynamics can be formulated in a number of different ways (1, 3–6, 9). Here, we present the formulation that is simplest and most appropriate to our method of empirical determination via weak values (4, 9). Being a complete interpretation of quantum mechanics, Bohmian mechanics applies to arbitrarily many particles and allows for internal degrees of freedom (such as spin). Here, we are concerned with a two-particle entangled state $|\Psi\rangle$. Denoting the positions (in one dimension for simplicity) of the two particles by x_1 and x_2 , the Bohmian velocity of particle 1 is (4, 9)

$$v_1(x_1, x_2) = \text{Re} \frac{\langle \Psi | \hat{v}_1 | x_1 \rangle | x_2 \rangle \langle x_2 | \langle x_1 | \Psi \rangle}{\langle \Psi | x_1 \rangle | x_2 \rangle \langle x_2 | \langle x_1 | \Psi \rangle} \quad (1)$$

where $\hat{v}_1 = (\hat{p}_1/m_1)$ is the velocity operator for particle 1.

The existence of entanglement entails counterintuitive effects in Bohmian mechanics, which ESSW used to attack the foundations of the theory as follows. Consider an experiment where a particle traverses a double-slit apparatus, thus preparing it in a state described by the double-slit wave function, $\psi(x_1; t = 0) = \frac{1}{\sqrt{2}}(\psi_u(x_1; 0) + \psi_l(x_1; 0))$. Here, the two wave functions $\psi_u(x_1; t)$ and $\psi_l(x_1; t)$ describe symmetric single-slit wave functions for slits centered at $x_1 = d/2$ and $x_1 = -d/2$, the specific form of which is not necessary for this discussion. Now, say the apparatus includes a WWM device—another quantum system that acts as a qubit memory, storing the single bit of information about which slit the particle goes through. This can be modeled by the following joint state of the double-slit particle and the WWM device at times $t > 0$

$$|\Psi(t)\rangle = \frac{1}{\sqrt{2}} \int dx_1 dx_2 |x_1\rangle |x_2\rangle [\Psi_u(x_1; t) \phi_H(x_2; t) |H\rangle + \Psi_l(x_1; t) \phi_V(x_2; t) |V\rangle] \quad (2)$$

Here, the WWM device is described as a particle with a spin degree of freedom, denoted (with forethought of the experiment described later in this text) by the kets $|H\rangle$ and $|V\rangle$ and a position x_2 . The spin degree of freedom provides the qubit that stores the WWM information, and the two states are correlated with the wave function for particle 1 initially localized at the upper and lower slit, respectively. The reason for choosing a spin degree of freedom for this role is that, unlike position, spin has no autonomous hidden variable assigned to it in standard Bohmian mechanics. [In some extensions to Bohmian mechanics, autonomous hidden variables are assigned to degrees of freedom other than position, such as spin (19). See Hiley and Callaghan (20) for a discussion in the context of the original ESSW proposal. To avoid the surreal trajectories of ESSW in the scenario we are considering, the hidden variable theory would have to assign a value to the particular spin observable with $|H\rangle$ and $|V\rangle$ as its eigenstates.] That is, Bohmian mechanics does not necessarily ascribe a definite value to the bit (H or V) storing the WWM information, and this is essential to the ESSW phenomenon. However, the position x_2 of particle 2 (which is ascribed a value in Bohmian mechanics) can be used to “read out” this WWM information, by sending particle 2 to different detectors depending on its spin state. Because these two states are orthogonal ($\langle H|V\rangle = 0$), it would be intuitive to conclude that such a measurement of the spin of particle 2 would indicate through which

slit particle 1 had gone (even though, in orthodox quantum mechanics, the particle has no trajectory and hence did not “go through” either slit).

In some situations, Bohmian mechanics accords with that intuition. If the WWM is read out as described above, at time $t_r > 0$, then for times $t < t_r$, $\phi_H(x_2; t)$ and $\phi_V(x_2; t)$ are identical, whereas for times $t > t_r$, $\phi_H(x_2; t)$ and $\phi_V(x_2; t)$ have disjoint support. If, at the time t_r , particle 1 is still in the near field of the double-slit apparatus, as in Fig. 1A, then the measurement outcome (the position of particle 2) is perfectly correlated with the origin (upper slit or lower slit) of each Bohmian trajectory. The velocity formula (Eq. 1) for particle 1 and $t > t_r$, as it traverses the apparatus toward the far field, gives $\text{Re} \left[\frac{-i\hbar \psi'_u(x_1; t)}{m\psi_u(x_1; t)} \right]$ or $\text{Re} \left[\frac{-i\hbar \psi'_l(x_1; t)}{m\psi_l(x_1; t)} \right]$, respectively, as expected from single-particle Bohmian mechanics.

ESSW, however, consider a situation where the readout via the position of particle 2 does not take place until after particle 1 has traversed the double-slit apparatus into the far field. In this case, while particle 1 traverses the apparatus, $\phi_H(x_2; t) = \phi_V(x_2; t)$ and the velocity formula (Eq. 1) is independent of x_2

$$v_1(x_1; t) = \frac{\hbar}{m} \text{Im} \left[\frac{\psi_u^*(x_1; t) \psi'_u(x_1; t) + \psi_l^*(x_1; t) \psi'_l(x_1; t)}{|\psi_u(x_1; t)|^2 + |\psi_l(x_1; t)|^2} \right] \quad (3)$$

This function is odd in x_1 because $\psi_u(-x_1; t) = \psi_l(x_1; t)$, for all t , by construction. Furthermore, the one-dimensional trajectories defined by using this velocity cannot cross because the velocity field is single-valued in x_1 . A consequence of these two properties is that no trajectory can

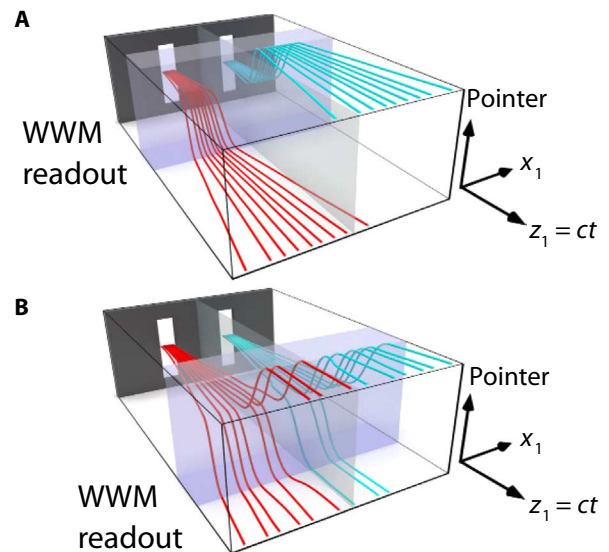


Fig. 1. Bohmian trajectories in a double-slit apparatus. (A and B) Conceptual diagram of the result of reading out the WWM in a double-slit apparatus in the near field (A) and in the midfield (B). Color indicates the slit of origin of a Bohmian trajectory, and vertical position indicates the result of the WWM (the position x_2 of the second, “pointer,” particle). When the WWM is read out in the near field, the Bohmian trajectories are perfectly correlated with the result of the WWM. When the WWM measurement is read out in the midfield, the Bohmian trajectories are only correlated with the WWM outcome near the edges of the diagram. Near the line of symmetry of the apparatus, both outcomes of the WWM are equally likely, regardless of which slit the Bohmian trajectory originates from.

cross the $x_1 = 0$ line. Thus, Bohmian mechanics in this situation predicts that, when particle 1 is detected in the far field, if $x_1 > 0$, then it must have come from the upper slit, and if $x_1 < 0$, then it must have come from the lower slit. Moreover, one can show that, in the far field, the position of particle 1 is almost completely uncorrelated with the spin of particle 2. Thus, upon detection of particle 1 anywhere in the far field, a measurement of particle 2 can yield either $|H\rangle$ or $|V\rangle$. A conceptualization of this is displayed in Fig. 1B in which the WWM readout actually occurs in the midfield for clarity. The trajectories corresponding to the measurement outcomes are “surreal” in the sense that the orthodox quantum intuition is that particle 2 should reliably carry the WWM information about which slit particle 1 “actually” went through, and yet we find that the trajectories predicted by Bohmian mechanics often fail to agree with the outcome of the WWM as read out via particle 2.

The resolution [presented by Hiley *et al.* (18)] of the apparent paradox is in the nonlocality of Bohmian mechanics. In Bohmian mechanics, the spin of particle 2 is described by a Bloch vector \mathbf{s}_2 that depends on the actual position of the two particles (21) in a manner exactly analogous to Eq. 1

$$\mathbf{s}_2(x_1, x_2; t) = \frac{\langle \Psi(t) | \hat{\mathbf{s}}_2 | x_1 \rangle \langle x_2 | \langle x_1 \rangle \langle x_2 | \Psi(t) \rangle}{\langle \Psi(t) | x_1 \rangle \langle x_2 \rangle \langle x_1 \rangle \langle x_2 | \Psi(t) \rangle} \quad (4)$$

where $\hat{\mathbf{s}} = (\sigma_x, \sigma_y, \sigma_z)$. We define $|H\rangle$ and $|V\rangle$ to be eigenstates of σ_z with eigenvalues $+1$ and -1 , respectively. Then, for the situation of Fig. 1A, Eq. 4 evaluates to $(1, 0, 0)^T$ or $(-1, 0, 0)^T$, depending on which slit particle 1 went through. For the situation in Fig. 1B (a delayed measurement), it evaluates to

$$\mathbf{s}_2(x_1, x_2; t) = \frac{(\psi_u^*(x_1; t) \langle H | + \psi_l^*(x_1; t) \langle V |) \hat{\mathbf{s}}_2 (|H\rangle \psi_u(x_1; t) + |V\rangle \psi_l(x_1; t))}{|\psi_u(x_1; t)|^2 + |\psi_l(x_1; t)|^2} \quad (5)$$

What we find here is that in Bohmian mechanics, contrary to the intuition one may have from orthodox quantum mechanics, the spin of particle 2 is not a constant of motion for propagation in free space. Rather, it evolves, as particle 1 moves along a trajectory. Thus, it is not surprising that in Bohmian mechanics, the spin of particle 2 is not a reliable indicator of which slit particle 1 went through. Similar unreliable behavior can result if the Welcher Weg information were stored in disjoint positional wave functions of the second particle, if those two wave functions are subsequently allowed to overlap, as in the experiment proposed by Braverman and Simon (11).

EXPERIMENT

Here, we perform an experiment using the spin of particle 2 as carrier of the Welcher Weg information, as per the above theory. We determine the trajectories of particle 1 in an operational manner that does not rely on a particular interpretation of quantum mechanics (9), as realized by Kocsis *et al.* (7), using weak measurements of velocity post-selected on the positions of the particles. The particles in this article are photons, as was the case in Kocsis *et al.* (7). Bohmian-like trajectories of massless spin 0 and spin 1 particles have been studied (22), but in the case of this experiment, we instead make use of the equivalence between the one-dimensional Schrodinger equation and the two-dimensional Helmholtz equation in the paraxial approximation. The evolution of the transverse position x and momentum k_x of a

single photon propagating close to the z direction has an exact mathematical correspondence with the quantum theory of a nonrelativistic particle of mass $m = \hbar\omega/c^2$ propagating in one dimension with position x and momentum $p = \hbar k_x$.

As described previously, the mapping out of a set of possible Bohmian trajectories for a particle requires a measurement of momentum followed by a measurement of position, repeated many times (that is, using an ensemble of identically prepared systems) to obtain averages, and repeated at many instants in time to connect the trajectory segments. It is the measurement of both position and momentum that makes mapping out the set of trajectories challenging: Quantum mechanics tells us that any measurement of momentum will necessarily disturb the position of the particle being measured. To circumvent this, we measure the momentum in such a way that a single shot yields virtually no information and causes virtually no disturbance, so that the subsequent strong measurement of position reveals [in the Bohmian interpretation (4)] the Bohmian position of the particle at the point where its momentum was measured (4, 9). Because the signal-to-noise ratio in any individual momentum measurement is so small, it is necessary to use a very large ensemble to obtain reliable averages. This technique of averaging such weak measurement results to obtain a so-called weak value (23) has been important in fundamental quantum experiments, including probing Hardy’s Paradox (24, 25), testing measurement-disturbance and complementarity relations (26–29), demonstrating violation of macrorealism (30, 31), and elucidating Feynman’s explanation of Bell correlations (32). It is not immediately obvious that this measurement will tell us anything about the Bohmian velocity of the particle being measured, because this velocity does not have the same statistics as the quantum mechanical momentum (divided by m). Nonetheless, it can be shown that this technique yields exactly (in the limit of infinite weakness) the Bohmian velocity for the particle at a given position (9). Thus, we can use our measurements of the average momentum for different positions and at different slices of time to reconstruct a set of Bohmian trajectories, as done by Kocsis *et al.* (7).

As stated, the particles in our experiment are photons and, in reference to the theory presented above, the spin operator $\hat{\mathbf{s}}$ corresponds to their polarization, with σ_z being diagonal in the H/V basis. The experimental apparatus is depicted in Fig. 2. We generate polarization-entangled photon pairs via type II downconversion (for details, see Materials and Methods). Photon 1 is sent through a 50-m-long single-mode fiber to a double-slit apparatus. The photon’s wave function is prepared in a double-slit superposition using a polarizing beamsplitter and a pair of prism mirrors, such that if the polarization of photon 1 is horizontal, it is prepared in the upper slit wave function, whereas if it is vertical, it is prepared in the lower slit wave function. These virtual slits are separated by 2.61 mm, and each has a root mean square width of 0.55 mm. The polarization of the photons in both paths is made the same, $|D\rangle = \frac{1}{\sqrt{2}}(|H\rangle + |V\rangle)$, by a set of half waveplates and a polarizer. Because of the initial polarization entanglement, the path of photon 1 is now entangled with the polarization of photon 2, as described in Eq. 2.

To perform a WWM on photon 1, we measure the polarization of photon 2 using a set of waveplates and polarizing beamsplitters. For details on how we perform measurements on photon 1 using a charge-coupled device (CCD) camera, in coincidence with measurements on photon 2, see Materials and Methods. Next, we weakly (23, 33) measured the velocity $v_1 = ck_x/|k|$ of photon 1, before strongly measuring

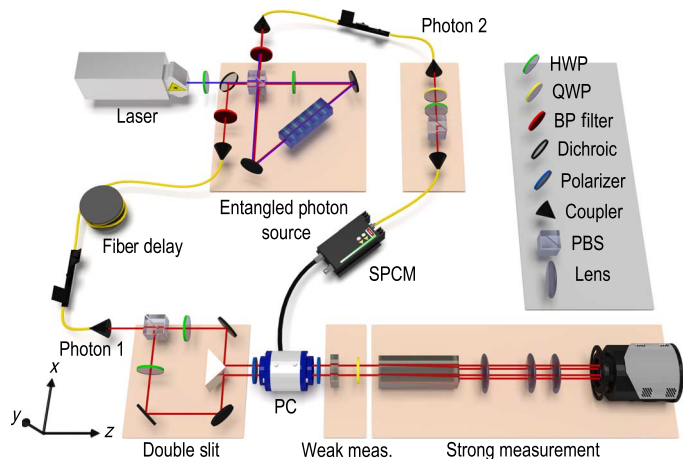


Fig. 2. Experimental setup for measuring Bohmian trajectories: The trajectories of a single photon (photon 1) are measured, postselected on a detection of another photon (photon 2) by a single photon counting module (SPCM). A Sagnac interferometer-based source of entangled photons prepares two photons in a maximally entangled state that are then spectrally filtered using two band-pass (BP) filters. Photon 1 is sent into a double-slit apparatus and immediately split at a polarizing beamsplitter (PBS) to prepare the double-slit wave function. The lower arm’s polarization is changed to match the upper arm using a half waveplate (HWP). Both upper and lower arms passed through a polarizer, a Pockels cell (PC), and another polarizer, to postselect upon the detection of photon 2. The transverse velocity of photon 1 is weakly measured using a 0.7-mm-thick piece of calcite with its optic axis oriented at 42° to the normal in the horizontal plane, followed by a quarter waveplate (QWP) and a beam displacer. Finally, the wave function of photon 1 is imaged in different planes using an imaging system composed of three lenses, and its position is measured using a single-photon cooled CCD. Photon 2 is sent through an HWP and a QWP, followed by a PBS to measure its polarization in different bases.

its position. To weakly measure the transverse velocity of photon 1, we coupled the k vector of photon 1 to its polarization using the angle-dependent birefringent phase shift produced by a piece of calcite (7) that is thin enough that spatial walk-off of the beam inside the crystal is negligibly small, but thick enough that the polarization rotation that the beam undergoes is measurable. The crystal’s optic axis was oriented in the horizontal plane; hence, photons with different transverse velocities experienced different indices of refraction and therefore received different phase shifts. The phase shift is well approximated over our range of incident angles (transverse momenta) by the linear expansion

$$\Phi(k_x) = \zeta \frac{k_x}{|\mathbf{k}|} + \Phi_0 \quad (6)$$

where the dimensionless coupling strength, ζ , was determined to be 550.2 ± 0.96 . This momentum-dependent phase shift serves to weakly correlate the photon’s momentum with its polarization. By measuring the polarization, a weak measurement of momentum is thus performed. The photon’s polarization was measured in the right-hand circular (R)/left-hand circular (L) basis [$|R/L\rangle = \frac{1}{\sqrt{2}}(|H\rangle \pm i|V\rangle)$] using a quarter waveplate oriented at 45° and a beam displacer, the combination of which displaces the L -polarized beam vertically relative to the

R . Using this polarization measurement, the photon’s weak-valued velocity takes on a particularly simple form (7)

$$\frac{v_1^w}{c} = \left(\frac{k_x}{|\mathbf{k}|} \right)^w = \frac{1}{\zeta} \left[\sin^{-1} \left(\frac{I_R - I_L}{I_R + I_L} \right) \right] \quad (7)$$

where $I_{R/L}$ is the ensemble average of the photon flux of the corresponding polarizations, measured at a particular point in space using the CCD camera. For details on how this point can be identified with the position of the photon at the time of the momentum measurement, see Materials and Methods.

RESULTS

In Fig. 3, we demonstrate the nonlocality present in Bohmian mechanics by showing that the trajectory of photon 1 is affected by the remote choice of how to measure photon 2. We measure the polarization of photon 2 in two different bases and postselect the measurement outcomes of photon 1 on a particular result, as described above. Defining states $|\psi^\Phi\rangle = \frac{1}{\sqrt{2}}(|H\rangle - e^{i\Phi}|V\rangle)$, the two different bases are $\{|\psi^0\rangle, |\psi^\pi\rangle\}$ and $\{|\psi^{\pi/2}\rangle, |\psi^{3\pi/2}\rangle\}$. All four final states $|\psi^\Phi\rangle$ are equally likely, and for each, we measure the set of trajectories that photon 1 follows. In this way, it is possible to plot a single trajectory beginning with the same initial conditions and show that the path depends on the choice of distant measurement. For clarity, the measured weak velocity distribution of photon 1 is also plotted in two planes to show the effect the postselection of photon 2 has on the motion of photon 1. Thus, one can see that even though the position of a particle is a locally defined hidden variable in Bohmian mechanics, the guiding equations that determine its possible trajectories are nonlocal.

Next, we aim to demonstrate the surreal behavior discussed by ESSW. We measure the trajectories of photon 1 without performing a postselection on photon 2. In this way, the position x_2 of photon 2 is uncorrelated with its polarization, giving Eq. 3 for the velocity of photon 1. To reject spurious background sources of photons, we actually do postselect on detecting photon 2, but we average over the two cases H and V by the weights with which these two outcomes occur (which are close to one-half). In fact, we get the same result regardless of the basis in which we measure the polarization of photon 2; thus, we average the data from three different bases, $|D/A\rangle$, $|R/L\rangle$, and $|H/V\rangle$, to most accurately calculate the velocity. The result in Fig. 4 shows that the particles are confined to the half-plane in which they begin, as ESSW predicted. In the far field and near the line of symmetry, the polarization of photon 2 is equally likely to be found to be H or V and therefore (one would naively think) the photon is equally likely to have come from the upper slit or the lower slit. Because each Bohmian trajectory originates from one or the other slit, these trajectories demonstrate the surreal behavior predicted by ESSW.

The apparent contradiction, however, is resolved by also measuring the polarization of photon 2 as a function of the position of photon 1. The measurements that we have performed on photon 2 ($|D/A\rangle$, $|R/L\rangle$, and $|H/V\rangle$), in correlation with the measurement of the position of photon 1, are sufficient to perform quantum state tomography (34) on the polarization of photon 2, along a trajectory of photon 1. Unlike the case of Eq. 1, it is not necessary to use a weak measurement of \hat{s}_z to determine Eq. 4, because \hat{s}_z commutes with the position of all particles at all times. Hence, we can make a strong measurement of

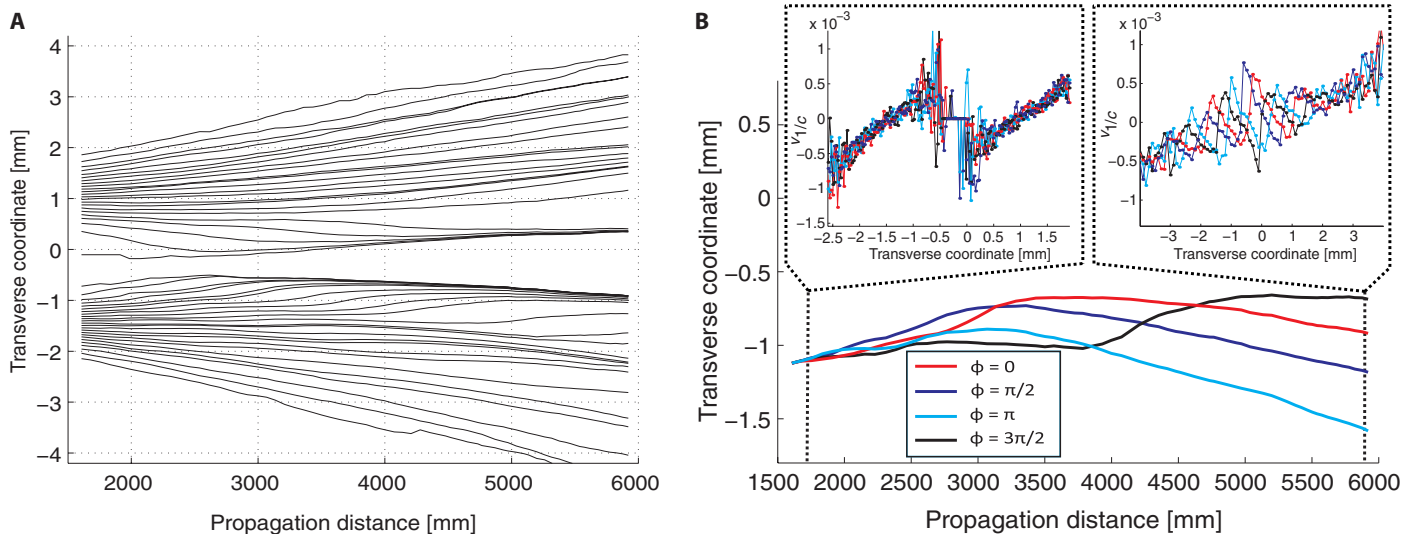


Fig. 3. Observation of nonlocality in Bohmian mechanics. (A) The reconstructed trajectories when photon 2 is found in the state $|A\rangle = \frac{1}{\sqrt{2}}(|H\rangle - |V\rangle)$. The trajectories are drawn over a range of $z = 1.7$ m to $z = 5.9$ m, using 67 different planes. The state of photon 1 after postselection contains no information about the state of photon 2, and thus, interference is observed. (B) A single postselected trajectory beginning at the same initial condition, $x = -1.12$ mm, for four different postselected polarization states of photon 2, $\frac{1}{\sqrt{2}}(|H\rangle - e^{i\Phi}|V\rangle)$, where $\Phi \in \{0, \pi/2, \pi, 3\pi/2\}$. The pairs $\{0, \pi\}$ and $\{\pi/2, 3\pi/2\}$ correspond to measuring the polarization of photon 2 in two different bases. (Inset) The weak velocity values measured at $z = 1.8$ m and $z = 5.9$ m. The velocity distributions are initially independent of phase shift applied to photon 2 but depend strongly on it in the far field. The error bars on the individual velocity measurements are consistent with the scatter observed but are not displayed because they detract from rather than enhance its clarity.

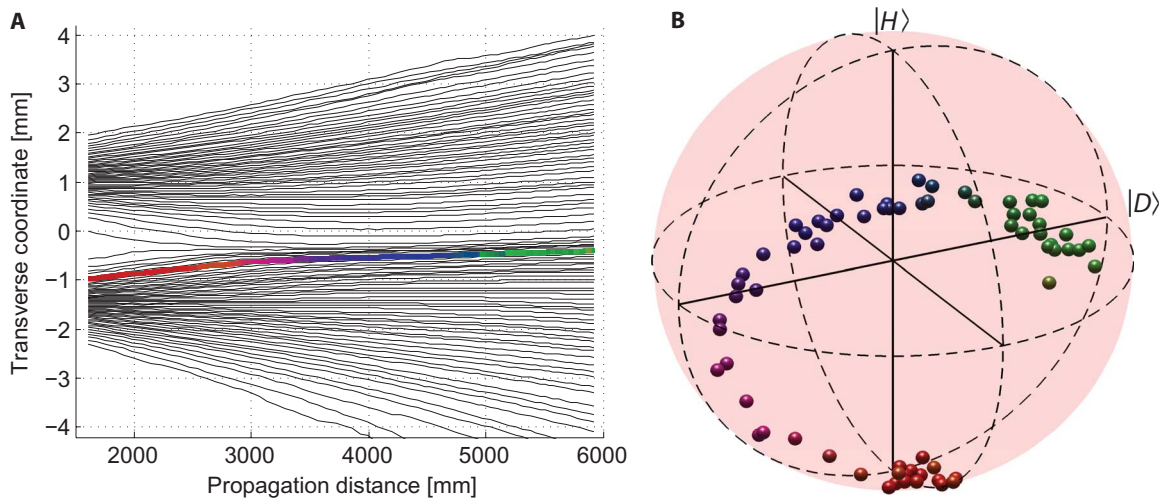


Fig. 4. Observation of surreal trajectories. (A) The set of reconstructed trajectories for photon 1 without postselection onto a particular polarization of photon 2, corresponding to the delayed WWM of ESSW. The trajectories are plotted over the range $z = 1.7$ m to $z = 5.9$ m, using 67 different planes. A single trajectory beginning at $x = -0.98$ mm is plotted with a thicker, colored line. (B) The polarization of photon 2, represented by its Bloch vector, as a function of the position of photon 1 as it traverses the colored trajectory plotted in (A). The polarization of photon 2 is calculated by performing quantum state tomography (34) on photon 2 and correlating those counts with the counts observed on the single-photon camera. The photons have been entangled such that if photon 1 were to be found in the lower slit, photon 2 would be vertically polarized. This is the case at the start of the single trajectory we consider. However, as photon 1 traverses the double slit, it enters a region where the wave function emanating from the upper slit (for which photon 2 is horizontally polarized) interferes with that from the lower slit, leading to nonlocal coupling between the motion of photon 1 and the polarization of photon 2. As a consequence, the polarization of photon 2 changes over time and its final state no longer faithfully records the WWM information about photon 1.

the polarization of particle 2, in the three directions (in different runs), conditioned on finding particle 1 at particular positions at particular times. The results of this measurement are plotted in Fig. 4. As a function of the progress of photon 1 along any trajectory that it may follow, the state of photon 2 changes. Initially, for a trajectory originating in the lower slit, photon 2 is found to be vertically polarized (indicating that the outcome of the WWM was “lower slit”). Further along this trajectory, the polarization of photon 2 gradually becomes less vertically polarized and ends up with polarization close to $|D\rangle$ (see Fig. 4). Thus, a WWM in the H/V basis (or “upper”/“lower” basis) for this photon, at this time, is equally likely to indicate that it came from the upper slit as from the lower slit.

DISCUSSION

We have verified the effect pointed out by ESSW that for a WWM with a delayed readout, Bohmian trajectories originating at the lower slit may be accompanied by WWM results associated with either the upper or the lower slit. However, this surreal behavior is merely the flip side of the nonlocality we also demonstrated. In Fig. 3, we showed that the trajectory of photon 1 depends on the choice of measurement (polarization basis) for photon 2. In Fig. 4, we see that the polarization of photon 2 depends on the choice of when (that is, at what point along the trajectory) to measure the position of photon 1. This nonlocality is due to the entanglement of the two photons, which, in Bohmian mechanics, makes their evolution inseparable even when the photons themselves are separated. Because entanglement is necessary for the delayed measurement scenario of ESSW, this nonlocal behavior is to be expected and is the reason for the surreal behavior they identify. Indeed, our observation of the change in polarization of a free space photon, as a function of the time of measurement of a distant photon (along one reconstructed trajectory), is an exceptionally compelling visualization of the nonlocality inherent in any realistic interpretation of quantum mechanics.

MATERIALS AND METHODS

To generate entangled photon pairs, we used a periodically poled KTP (potassium titanyl phosphate) crystal embedded in a polarization Sagnac interferometer (35–37). The source generates entangled photon pairs (at a rate of approximately 25,000 pairs/s and a coupling efficiency of $\sim 10\%$) in a state ρ that has fidelity $F = \langle \phi^+ | \rho | \phi^+ \rangle = 99.04 \pm 0.02\%$ with the Bell state $|\phi^+\rangle = \frac{1}{\sqrt{2}}(|HH\rangle + |VV\rangle)$, where H and V correspond to horizontal and vertical polarization, respectively.

To perform measurements on photon 1 in coincidence with measurements on photon 2, we triggered a Pockels cell to block photon 1 unless photon 2 was detected. The Pockels cell is set to apply a π phase shift to the vertical polarization upon receiving a TTL (transistor-transistor logic) pulse from the single-photon counter. This phase shift converts the polarization of photon 1 from $|D\rangle$ to $|A\rangle = \frac{1}{\sqrt{2}}(|H\rangle - |V\rangle)$, allowing it to pass through a polarizer following the cell. That is, the detection of photon 2 effectively opens a fast shutter for photon 1, enabling coincidence detection on the nanosecond time scale using a single-photon cooled CCD (Andor iDus) whose response time is six orders of magnitude slower.

To obtain the data for the trajectories, photon 1 was imaged in different planes using two fixed lenses (with focal lengths of 10 and 15 cm) and a third translatable lens (with a focal length of 2.5 cm) in between them. The magnification and imaging distance of the imaging system (consisting of the three lenses and the CCD camera) were determined by sweeping the position of the middle lens with one slit blocked and the weak measurement calcite removed. The magnification of the system was then given by $1/x$, where x is the distance from the imaged spot to the line of symmetry of the imaging system. The imaging distance as a function of the lens position was determined by stretching the calibration images (by a factor inversely proportional to the magnification) so that the true image can be extracted for each position of the middle lens. Finally, the width of the spot in the true image was determined, from which the imaging distance can be determined using Gaussian beam propagation equations. Note that because Bohmian trajectories do not cross in one dimension, these propagation equations also relate the Bohmian position of the particle at the plane where the momentum measurement was performed with that in the plane where it was imaged.

REFERENCES AND NOTES

1. D. Bohm, A suggested interpretation of the quantum theory in terms of “hidden” variables. I. *Phys. Rev.* **85**, 166–179 (1952).
2. D. Bohm, A suggested interpretation of the quantum theory in terms of “hidden” variables. II. *Phys. Rev.* **85**, 180–193 (1952).
3. D. Bohm, B. Hiley, *The Undivided Universe: An Ontological Interpretation of Quantum Theory* (Routledge, New York, 1993).
4. D. Dürr, S. Goldstein, N. Zanghi, *Quantum Physics Without Quantum Philosophy* (Springer, Heidelberg, 2013).
5. L. de Broglie, *Une tentative d’interprétation causale et non linéaire de la mécanique ondulatoire (la théorie de la double solution)* (Gauthier-Villars, Paris, 1956).
6. P. Holland, *Quantum Theory of Motion: Account of the de Broglie-Bohm Causal Interpretation of Quantum Mechanics* (Cambridge Univ. Press, Cambridge, 1995).
7. S. Kocsis, B. Braverman, S. Ravets, M. J. Stevens, R. P. Mirin, L. K. Shalm, A. M. Steinberg, Observing the average trajectories of single photons in a two-slit interferometer. *Science* **332**, 1170–1173 (2011).
8. R. P. Feynman, Space-time approach to non-relativistic quantum mechanics. *Rev. Mod. Phys.* **20**, 367–387 (1948).
9. H. M. Wiseman, Grounding Bohmian mechanics in weak values and bayesianism. *New J. Phys.* **9**, 165–177 (2007).
10. J. S. Bell, On the Einstein-Podolsky-Rosen paradox. *Physics* **1**, 195–200 (1964).
11. B. Braverman, C. Simon, Proposal to observe the nonlocality of Bohmian trajectories with entangled photons. *Phys. Rev. Lett.* **110**, 060406 (2013).
12. B.-G. Englert, M. O. Scully, G. Süssmann, H. Walther, Surrealistic Bohm trajectories. *Z. Naturforsch.* **47a**, 1175–1186 (1992).
13. M. O. Scully, Do Bohm trajectories always provide a trustworthy physical picture of particle motion? *Phys. Scr.* **1998**, T76 (1998).
14. C. Dewdney, L. Hardy, E. J. Squires, How late measurements of quantum trajectories can fool a detector. *Phys. Lett. A* **184**, 6–11 (1993).
15. D. Dürr, W. Füsseder, S. Goldstein, N. Zanghi, Comment on “Surrealistic Bohm trajectories”. *Z. Naturforsch.* **48a**, 1261–1262 (1993).
16. B.-G. Englert, M. O. Scully, G. Süssmann, H. Walther, Reply to Comment on “Surrealistic Bohm trajectories”. *Z. Naturforsch.* **48a**, 1263–1264 (1993).
17. L. Vaidman, The reality in Bohmian quantum mechanics or can you kill with an empty wave bullet? *Found. Phys.* **35**, 299–312 (2005).
18. B. J. Hiley, R. Callaghan, O. Maroney, Quantum trajectories, real, surreal or an approximation to a deeper process? *ArXiv:quant-ph/0010020* (2000).
19. P. R. Holland, Causal interpretation of a system of two spin-1/2 particles. *Phys. Rep.* **169**, 293–327 (1988).
20. B. J. Hiley, R. E. Callaghan, Delayed-choice experiments and the Bohm approach. *Phys. Scr.* **74**, 336–348 (2006).
21. C. Dewdney, P. R. Holland, A. Kyrianiadis, J. P. Vigiier, Spin and non-locality in quantum mechanics. *Nature* **336**, 536–544 (1988).
22. P. Ghose, A. S. Majumdar, S. Guha, J. Sau, Bohmian trajectories for photons. *Phys. Lett. A* **290**, 205–213 (2001).

23. Y. Aharonov, D. Z. Albert, L. Vaidman, How the result of a measurement of a component of the spin of a spin-1/2 particle can turn out to be 100. *Phys. Rev. Lett.* **60**, 1351–1354 (1988).
24. J. S. Lundeen, A. M. Steinberg, Experimental joint weak measurement on a photon pair as a probe of Hardy's paradox. *Phys. Rev. Lett.* **102**, 020404 (2009).
25. K. Yokota, T. Yamamoto, M. Koashi, N. Imoto, Direct observation of Hardy's paradox by joint weak measurement with an entangled photon pair. *New J. Phys.* **11**, 033011 (2009).
26. R. Mir, J. S. Lundeen, M. W. Mitchell, A. M. Steinberg, J. L. Garretson, H. M. Wiseman, A double-slit 'which-way' experiment on the complementarity–uncertainty debate. *New J. Phys.* **9**, 287–297 (2007).
27. L. A. Rozema, A. Darabi, D. H. Mahler, A. Hayat, Y. Soudagar, A. M. Steinberg, Violation of Heisenberg's measurement–disturbance relationship by weak measurements. *Phys. Rev. Lett.* **109**, 100404 (2012).
28. M. M. Weston, M. J. W. Hall, M. S. Palsson, H. M. Wiseman, G. J. Pryde, Experimental test of universal complementarity relations. *Phys. Rev. Lett.* **110**, 220402 (2013).
29. F. Kaneda, S.-Y. Baek, M. Ozawa, K. Edamatsu, Experimental test of error-disturbance uncertainty relations by weak measurement. *Phys. Rev. Lett.* **112**, 020402 (2014).
30. J. Dressel, C. J. Broadbent, J. C. Howell, A. N. Jordan, Experimental violation of two-party Leggett-Garg inequalities with semiweak measurements. *Phys. Rev. Lett.* **106**, 040402 (2011).
31. M. E. Goggin, M. P. Almeida, M. Barbieri, B. P. Lanyon, J. L. O'Brien, A. G. White, G. J. Pryde, Violation of the Leggett–Garg inequality with weak measurements of photons. *Proc. Natl. Acad. Sci. U.S.A.* **108**, 1256–1261 (2011).
32. B. L. Higgins, M. S. Palsson, G. Y. Xiang, H. M. Wiseman, G. J. Pryde, Using weak values to experimentally determine "negative probabilities" in a two-photon state with Bell correlations. *Phys. Rev. A* **91**, 012113 (2015).
33. N. W. M. Ritchie, J. G. Story, R. G. Hulet, Realization of a measurement of a "weak value". *Phys. Rev. Lett.* **66**, 1107–1110 (1991).
34. D. F. V. James, P. G. Kwiat, W. J. Munro, A. G. White, Measurement of qubits. *Phys. Rev. A* **64**, 052312 (2001).
35. T. Kim, M. Fiorentino, F. N. C. Wong, Phase-stable source of polarization-entangled photons using a polarization Sagnac interferometer. *Phys. Rev. A* **73**, 012316 (2006).
36. F. N. C. Wong, J. H. Shapiro, T. Kim, Efficient generation of polarization-entangled photons in a nonlinear crystal. *Laser Phys.* **16**, 1517–1524 (2006).
37. A. Fedrizzi, T. Herbst, A. Poppe, T. Jennewein, A. Zeilinger, A wavelength-tunable fiber-coupled source of narrowband entangled photons. *Opt. Express* **15**, 15377–15386 (2007).

Acknowledgments: We thank C. Simon for useful discussions and B. Braverman for both useful discussions and helpful code. We also thank A. Stummer for designing the coincidence circuit. **Funding:** D.H.M., L.R., K.F., L.V., K.J.R., and A.S. acknowledge support from the Natural Sciences and Engineering Research Council of Canada and the Canadian Institute for Advanced Research. D.H.M., L.R., and A.S. acknowledge support from Northrop Grumman Aerospace Systems. K.F., L.V., and K.J.R. also acknowledge Industry Canada, Canada Research Chairs, the Canada Foundation for Innovation, and the Ontario Centres of Excellence. D.H.M. acknowledges additional support from the Walter C. Sumner Foundation. H.M.W. acknowledges support from the Australian Research Council Discovery Project DP140100648. **Author contributions:** D.H.M., L.R., H.M.W., and A.S. designed the experiment. D.H.M. and L.R. carried out data collection and analysis. K.F., L.V., and K.J.R. constructed and operated the source of photon pairs and aided in the alignment of the Pockels cell. All authors contributed to writing the paper, including preparing figures. **Competing interests:** The authors declare that they have no competing interests. **Data and materials availability:** All data needed to evaluate the conclusions in the paper are present in the paper and/or the Supplementary Materials. Additional data are available from the authors upon request.

Submitted 15 October 2015

Accepted 5 December 2015

Published 19 February 2016

10.1126/sciadv.1501466

Citation: D. H. Mahler, L. Rozema, K. Fisher, L. Vermeyden, K. J. Resch, H. M. Wiseman, A. Steinberg, Experimental nonlocal and surreal Bohmian trajectories. *Sci. Adv.* **2**, e1501466 (2016).

This article is published under a Creative Commons license. The specific license under which this article is published is noted on the first page.

For articles published under [CC BY](#) licenses, you may freely distribute, adapt, or reuse the article, including for commercial purposes, provided you give proper attribution.

For articles published under [CC BY-NC](#) licenses, you may distribute, adapt, or reuse the article for non-commercial purposes. Commercial use requires prior permission from the American Association for the Advancement of Science (AAAS). You may request permission by clicking [here](#).

The following resources related to this article are available online at <http://advances.sciencemag.org>. (This information is current as of October 17, 2016):

Updated information and services, including high-resolution figures, can be found in the online version of this article at:

<http://advances.sciencemag.org/content/2/2/e1501466.full>

This article **cites 32 articles**, 2 of which you can access for free at:

<http://advances.sciencemag.org/content/2/2/e1501466#BIBL>

Science Advances (ISSN 2375-2548) publishes new articles weekly. The journal is published by the American Association for the Advancement of Science (AAAS), 1200 New York Avenue NW, Washington, DC 20005. Copyright is held by the Authors unless stated otherwise. AAAS is the exclusive licensee. The title *Science Advances* is a registered trademark of AAAS